Paper published on:
Solar Energy vol. 131 (2016), pages: 199–207
DOI: 10.1016/j.solener.2016.02.045
http://www.sciencedirect.com/science/article/pii/S0038092X16001547

Compositional dependence of optical properties of zirconium, hafnium and tantalum carbides for solar absorber applications

Elisa Sani*[a], Luca Mercatelli[a], Marco Meucci[a], Andrea Balbo[b], Laura Silvestroni[c] and Diletta Sciti[c]
[a]*CNR-INO National Institute of Optics, Largo E. Fermi, 6, I-50125 Firenze, Italy*
[b]*Corrosion and Metallurgy Study Centre "Aldo Daccò", Engineering Department, University of Ferrara, G. Saragat 1, Ferrara 44122, Italy*
[c]*CNR-ISTEC, Institute of Science and Technology for Ceramics, Via Granarolo 64, I-48018 Faenza (Italy)*
** Corresponding author, email: elisa.sani@ino.it*

ABSTRACT
Besides ultra-refractoriness and favorable mechanical and chemical characteristics, carbides of early transition metals show intrinsic spectral selectivity, making them appealing for high-temperature solar absorber applications. However these kinds of ceramics can be produced using many processing methods resulting in different compositions, density and surface finishing. Thus the present work reports on the systematic study of microstructural, mechanical and optical properties of dense zirconium, hafnium and tantalum carbides as a function of the sintering method (high pressure or pressureless), implying use of 10 or 20 vol% of $MoSi_2$ as sintering aid. The spectral hemispherical reflectance of Zr-, Hf- and Ta-carbides has been measured in the 0.25-16.5 μm wavelength range and correlated to the surface microstructure and roughness. Room and high temperature fracture strength has been measured as well.

Keywords: carbides; Ultra-High Temperature Ceramics; optical properties; solar absorbers; solar plants; concentrating solar power.

1. Introduction

Concentrating solar power is one of the most promising renewable energy technologies. Sun radiation is collected and concentrated upon a receiver (e.g. a pipe, a surface,..). A heat-carrying fluid transports the heat to a power station. The heat is used to produce steam that drives an electricity turbo-generation unit [1]. The obtainable efficiency thus increases with increasing operating temperature.

The solar receiver is a key element and a large effort is devoted to the development of novel receiver architectures able to raise the plant operating temperature [2-5]. As for the receiver material, up to now the research has been addressed mainly to refractory ceramics, like silicon carbide (SiC) [6-8], alumina [9] and, more recently, ultra-high temperature carbides and borides [10-18] and black zirconia [19]. Blackbody-like absorbers (e.g. SiC) show high radiation losses, thus corrective actions have been recently proposed including, for instance, the addition of external reflectors [20], which, however, considerably increase the system complexity. Moreover, the importance of spectral selectivity in high temperature solar absorbers has been studied in the literature [21], and the simplest approach in this case is identifying materials with intrinsic selectivity properties.

Recent studies on ultra-high temperature ceramics (UHTCs) have shown that carbides and borides of zirconium, hafnium and tantalum possess, besides other favorable characteristics like high thermal conductivity high hardness and strength and the highest melting points of any known

Paper published on:
Solar Energy vol. 131 (2016), pages: 199–207
DOI: 10.1016/j.solener.2016.02.045
http://www.sciencedirect.com/science/article/pii/S0038092X16001547

material, also good spectral selectivity and low emittance at high temperatures [10-18]. The main weakness of these carbides is their poor resistance to oxidation, so they are primarily proposed for operation in vacuum, like in the device described in [22], or under inert atmosphere. However, it should be emphasized that the introduction of secondary phases able to produce silica-based glass (like SiC, $MoSi_2$, $TaSi_2$ and all transition-metal silicides) greatly improves their oxidation resistance [23,24].

UHTCs can be produced through a variety of processing methods, compositions and with full density or tailored porosities. Previous works on optical properties of UHT-carbides was focused on the screening of different compositions, in terms of type and amount of secondary phases, sintering aids, levels of porosity, etc. One study [12] demonstrated the intrinsic selectivity of refractory carbides as a general characteristic. However, drawing precise relationships between surface, microstructure and optical spectra was not feasible due to the non-systematic change of microstructural features. Other works put in evidence the lower emissivity of these carbides with respect to silicon carbide, which is again related to their spectral selectivity. For instance, the total hemispherical emissivity of ZrC, HfC, TaC at 1200 K lies in the 0.3-0.4 range, against 0.8 of SiC at the same temperature [10,11]. These values can notably increase with increase of the surface roughness/porosity. For instance, for HfC-based materials, a porosity increase from 5 to 30 vol% led to significant gain of emissivity from 0.4 to 0.55 [15].

A precise knowledge of factors affecting optical properties of these ceramic is of great importance for material optimization in view of solar absorber applications. Therefore, the aim of this work is a systematic study of optical properties amongst dense ZrC, HfC and TaC, containing 10 and 20 vol% of $MoSi_2$ as sintering aid and controlled surface roughness.

2. Experimental

Commercial powders were used for the preparation of materials: cubic ZrC (Grade B, H.C. Starck, Germany), mean grain size 3.8 μm, impurities (wt%) C:1.5, O:0.6, N:0.8, Fe:0.05, Hf:2.0; cubic HfC (Cerac Inc., USA), mean grain size 1.04 μm, impurities (wt%) Zr:<0.6, O:0.35, Cd:0.002; cubic TaC (Cerac Inc., USA), mean grain size 1.21 μm, impurities (wt%) Ti:0.04, Nb:0.03, Na:0.03, Fe:0.02, Ca:0.01; tetragonal $MoSi_2$ (Aldrich, USA) mean grain size 2.8 μm, impurities (wt%) O:1.

Matrix and additive were weighed in the proper amount, ultrasonically treated and mixed through mechanical mixing for 24 h in absolute ethanol using ZrO_2 milling media. Subsequently the slurries were dried in a rotary evaporator and sieved through 250 μm screen. 30 to 45 mm-diameter pellets were green shaped by uniaxial pressing with 20 MPa. The pellets to be sintered by hot pressing were directly placed in the furnace and hot pressed in low vacuum (~100 Pa) using an induction-heated graphite die with an uniaxial pressure of 30 MPa during the heating and a dwell at the maximum temperature set on the basis of the shrinkage curve, as reported in Table 1. On the other hand, the pellets to be sintered without applied pressure were preliminarily consolidated by cold isostatic pressing at 25 MPa and then sintered in a graphite furnace (Astro industries Inc., Santa Barbara, USA) with a heating rate of 600°C/h under flowing argon atmosphere (~0.1 MPa) at 1950°C, as indicated in Table 1. For all composites, free cooling followed.

On sintered materials, the bulk densities were measured by Archimedes' method and confirmed by SEM inspection.

The microstructure of sintered ceramics was analysed on fractured and polished surfaces by scanning electron microscopy (FE-SEM, Carl Zeiss Sigma NTS Gmbh, Oberkochen, DE) and energy dispersive x-ray spectroscopy (EDS, INCA Energy 300, Oxford instruments, UK). Quantitative calculations of the microstructural parameters, like residual porosity, mean grain size and secondary phase content, were carried out via image analysis with commercial software package (Image-Pro Plus® version 7, Media Cybernetics, Silver Springs, MD, USA).

Paper published on:
Solar Energy vol. 131 (2016), pages: 199–207
DOI: 10.1016/j.solener.2016.02.045
http://www.sciencedirect.com/science/article/pii/S0038092X16001547

A standard procedure for surface finishing was adopted to exclude any influence of polishing time, pressure and grade on the optical spectrum recorded. The optical surface of all specimens was polished using diamond paste from 30 μm down to 0.25 μm grain size.

The topological characterization of the surfaces was then carried out with a non-contact 3D profilometer (Taylor-Hobson CCI MP) on two areas of 0.08 x 1 cm^2 at the centre of each sample and the topography data were analysed using commercial software (Talymap 6.2). The evaluation of 2D texture parameters (average roughness, Ra, and maximum distance between peak and valley, Rt) was performed on 4 different profiles (2 for each area) extracted from the 3D data and the gaussian filter (λc) for the separation of the roughness and waviness components was set according to the ISO 4288:2000. The 2D parameters were calculated as average of estimated values on all sampling lengths over each profile.

Mechanical properties of carbides were measured in previous works [23,24] and the procedure is here described for the sake of clarity. It has to be mentioned that, for the hot pressed samples, values of strength were determined on compositions with slightly higher content of $MoSi_2$, e.g. 15 vol% [23]. It is assumed that a decrease of $MoSi_2$ from 15 to 10 vol% did not significantly affect the flexural strength up to 1500 K.

The room temperature flexural strength was measured according to the existing standard for advanced ceramics, method ENV 843-1, on chamfered bars with dimensions, 25 x 2.5 x 2.0 mm^3 (length by width by thickness, respectively), using a fully-articulated steel four-point fixture with a lower span of 20 mm and an upper span of 10 mm using a screw-driven load frame (Zwick-Roell mod. Z050). The high temperature strength was measured according to the ENV 820-1 standard, in partially protective Argon atmosphere in order to reduce any oxidation effect and using a semi-articulated alumina four-point fixture (Instron mod. 1195). For the high-temperature tests, a soaking time of 18 min was set to reach thermal equilibrium. For each material, five samples were tested.

The hemispherical reflectance spectra were acquired using two instruments: a double-beam spectrophotometer (Lambda900 by Perkin Elmer) equipped with a Spectralon®-coated integration sphere for the 0.25-2.5 μm wavelength region and a Fourier Transform spectrophotometer (FT-IR "Excalibur" by Bio-Rad) equipped with a gold-coated integrating sphere and a liquid nitrogen-cooled detector for the range 2.5-16.5 μm.

Label	Matrix	$MoSi_2$	Sintering	T,t,P	Bulk density	Rel. ρ	m.g.s.	Sec. phases by SEM-EDS	σRT	σ1500
		Vol%		°C,min,MPa	g/cm^3	%	μm	Vol%	MPa	MPa
ZCM10	ZrC	10	HP	1930,14,35	6.6	>99.5	5.1±1.4	1.5 $MoSi_2$, 5 SiC	~470*	~330(1)
ZCM20		20	PLS	1950,60,- Ar	6.4	>97	7.6±2.1	11 $MoSi_2$, 5 SiC, 3 Zr_xSi_y	270±10	160±10
HCM10	HfC	10	HP	1900,10,35	11.79	>99.5	1.5±0.4	5 SiC, 6 HfO_2, 3 $MoSi_2$, 1 Mo_5Si_3	~420*	~290(1)
HCM20		20	PLS	1950,60,- Ar	10.36	94	1.9±0.4	5 $MoSi_2$, 1 Hf-Si-C	380±70	350±80
TCM10	TaC	10	HP	1850,10,30	13.28	>99.5	1.5±0.4	6 $MoSi_2$, 3 SiC/SiO_2	~900*	~500(1)
TCM20		20	PLS	1950,60,- Ar	12.66	98.5	5.1±1.5	13 $MoSi_2$, 2 SiC/SiO_2, 1 Ta_xSi_y	590±60	320±40

PLS: pressureless sintering
HP: hot pressing
*Data collected on hot pressed compositions, but containing 15 vol% $MoSi_2$ instead of 10 vol% [23].

Table I: *Composition, sintering parameters (T: Temperature, t: dwell at T, P: applied pressure), final and relative densities (ρ), carbide mean grain size (m.g.s.), secondary phases and thermo-mechanical properties of the UHTCs sintered with $MoSi_2$. σ - 4-point flexural strength at room temperature or at 1500K in Argon.*

Paper published on:

Solar Energy vol. 131 (2016), pages: 199–207
DOI: 10.1016/j.solener.2016.02.045
http://www.sciencedirect.com/science/article/pii/S0038092X16001547

3. Results

3.1 Surface microstructure of dense UHTCs

To correlate optical spectra to compositional characteristics, SEM image analysis was carried out on the optically investigated surfaces.

3.1.1 ZrC-based composites (ZCM)

HP ZrC- 10 $MoSi_2$ (ZCM10) - This material started to shrink at around 1700°C and achieved a final density of 6.6 g/cm^3 at 1900°C for 12 min. SEM images taken on the optical surface (Fig. 1a) revealed almost no residual porosity. The bright phase corresponds to ZrC grains, which have a mean grain size of 5 μm and a rounded equiaxial shape, the dark agglomerates are SiC particles, often embedded into $MoSi_2$, that appears as a grey phase with irregular shape. The formation of SiC was attributed to the reaction between $MoSi_2$ and residual carbon present as an impurity in the starting ZrC powder (1.5 wt%) [25].

PLS ZrC - 20 $MoSi_2$ (ZCM20) – This composite was sintered at 1950°C achieving a relative density above 97% of the theoretical one. Accordingly, around 2% of small pores were recognized on the polished surface upon SEM inspection. Zirconium carbide grains in Fig. 1b have a squared shape and a mean grain size of 7.6 μm, see Table I. In the insets of Fig. 1b, $MoSi_2$ is the light grey phase with irregular shape, arranged among the matrix particles. By image analysis the presence of about 5.1 vol% of SiC was confirmed, with dark contrast and always next to $MoSi_2$ phase, whose amount was reduced to 11.3 vol%, see Table I. At the apical parts of $MoSi_2$ phase (see the upper inset of Fig. 1b), mixed Zr_xSi_y phases with different stoichiometry were detected by EDS, which showed very low dihedral angles; these phase were as large as several micrometers and were estimated to be around 3-4 vol%. These surface characteristics were coherent with those the bulk.

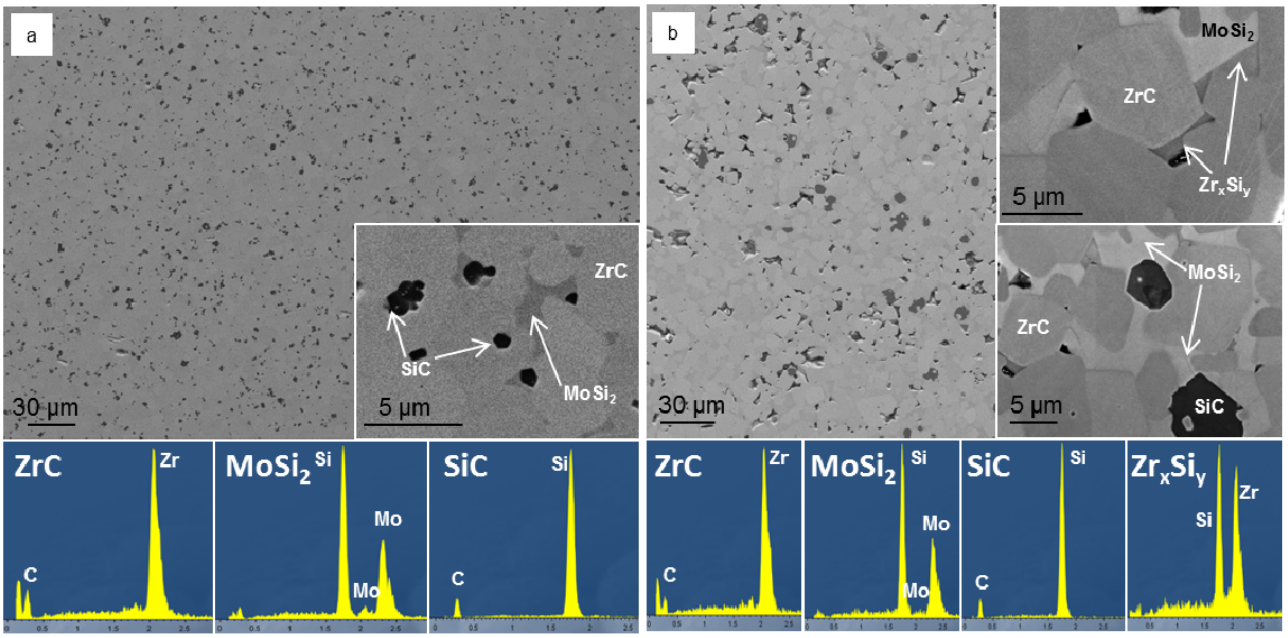

Figure 1: *SEM images of the microstructure of ZrC-based composites sintered by a) hot pressing and 10 vol% of $MoSi_2$, b) pressureless sintering and 20 vol% of $MoSi_2$ with EDS spectra of the various phases.*

Paper published on:
Solar Energy vol. 131 (2016), pages: 199–207
DOI: 10.1016/j.solener.2016.02.045
http://www.sciencedirect.com/science/article/pii/S0038092X16001547

3.1.2 HfC-based composites (HCM)

HP HfC- 10 $MoSi_2$ (HCM10) - This material was densified at 1900°C for 10 min (Table I). SEM analyses on the optical surface and in the bulk were in agreement with density measurements, indicating a residual porosity below 1%. A fine-grained microstructure was detected on the polished section (Fig. 2a), with HfC mean grain size around 1.5 µm. The white phase scattered throughout the surface in Fig. 2a was identified as HfO_2, around 5.6%. $MoSi_2$ phase, left in amount around 3 vol%, had an irregular shape with concave dihedral angles and showed the tendency to encase other secondary phases, like SiC or SiCO particles with dark contrast (about 5 vol%). In addition, about 1 vol% of mixed silicide with 5:3 stoichiometry, presumably based on Mo_5Si_3, was detected by EDS analysis.

PLS HfC- 20 $MoSi_2$ (HCM20) - Also this composite was sintered at 1950°C in the pressureless furnace, but the final relative density was around 94% of the theoretical one. The surface of the pellet showed about 12 vol% of porosity, due to partial $MoSi_2$ removal during the polishing procedure (Fig. 2b), resulting in a net $MoSi_2$ amount below 5 vol%. After sintering the mean grain size of HfC was about 2 µm, with homogeneous size and shape and no abnormal grown grains. Images of the polished optical surface (Fig. 2b) revealed $MoSi_2$ phase regularly dispersed in the HfC matrix. Among the faceted HfC grains, mixed products were detected by EDS analysis, containing Hf, Si, and C (inset of Fig. 2b). The amount of this phase was calculated to be below 1 vol% by image analysis. Additional SEM inspections in the bulk, revealed a fully dense material containing the nominal amount of $MoSi_2$.

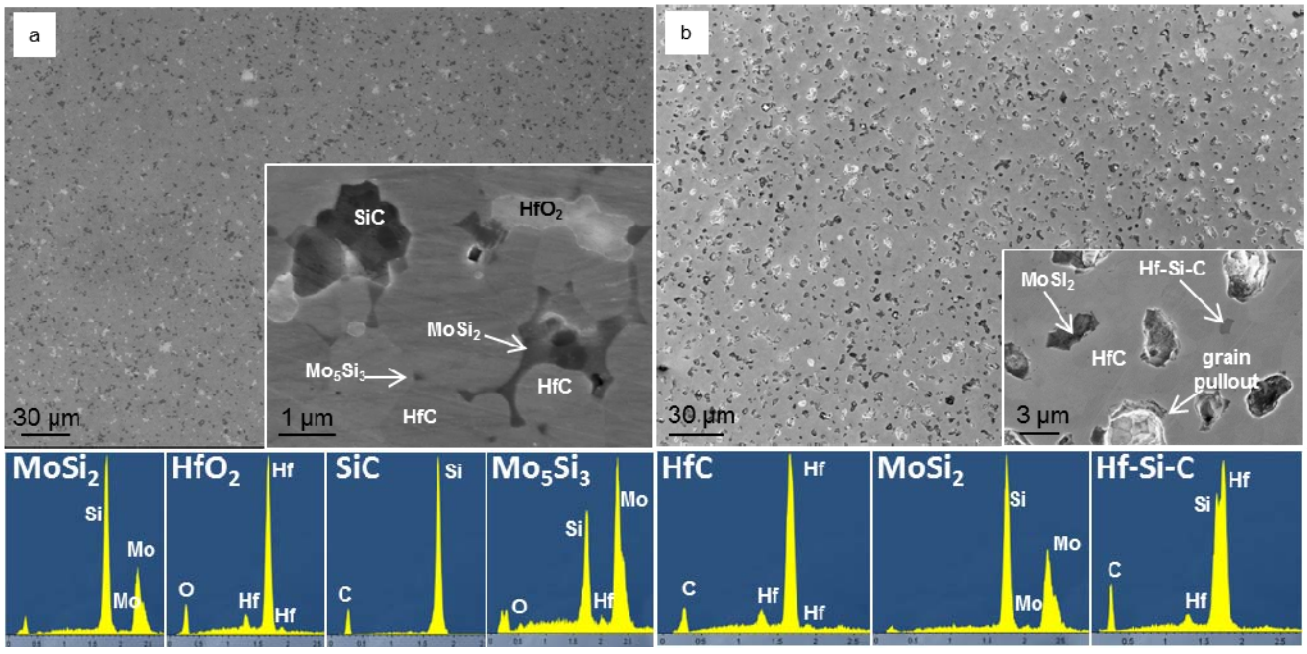

Figure 2: *SEM images of the surface of HfC-based composites sintered by a) hot pressing and 10 vol% of $MoSi_2$ and b) pressureless sintering and 20 vol% of $MoSi_2$ with EDS spectra of the various phases.*

3.1.3 TaC-based composites

HP TaC- 10 $MoSi_2$ (TCM10) - Compared to ZrC and HfC sintered with $MoSi_2$, shrinkage of TCM10 started at lower temperature, 1690°C and was completed at 1850°C (Table I). The polished surface (Fig. 3a) showed that this composite had a fine and homogenous microstructure with TaC mean grain size around 1.5 µm and the $MoSi_2$ pockets, reduced to an amount around 6 vol%, with

Paper published on:
Solar Energy vol. 131 (2016), pages: 199–207
DOI: 10.1016/j.solener.2016.02.045
http://www.sciencedirect.com/science/article/pii/S0038092X16001547

mean grain size around 1 μm, but ranging from 0.1 to 4.8 μm. Good adhesion was found between matrix and secondary phase. Little or no porosity was detected by SEM. Considerable amount of SiC or silica pockets was observed in the microstructure, about 3 vol%, as verified by image analysis (see the inset in Fig. 3a). Since SiC grains were generally found embedded in SiO_2 glassy pockets, it was difficult to avoid the C or O signal in the EDS spectra reported in Fig. 3.

PLS TaC- 20 $MoSi_2$ (TCM20) - This material, sintered at 1950°C, resulted in a relative density around 98%, Table I, but SEM inspection revealed a fully dense microstructure. This discrepancy could be due to the formation of 1-2% of lower-density phases, such as Si-O-C, as pointed out in the inset of Fig. 3b. The matrix grains had a squared shape and were quite homogeneous in size, around 5 μm. $MoSi_2$, in amount around 13 vol%, appeared in the typical look as the previous materials, with irregular shape and very low dihedral angles. In the apical part of $MoSi_2$, at the interface with the matrix, a mixed Ta_xSi_y phase was observed and estimated to be around 1 vol%.

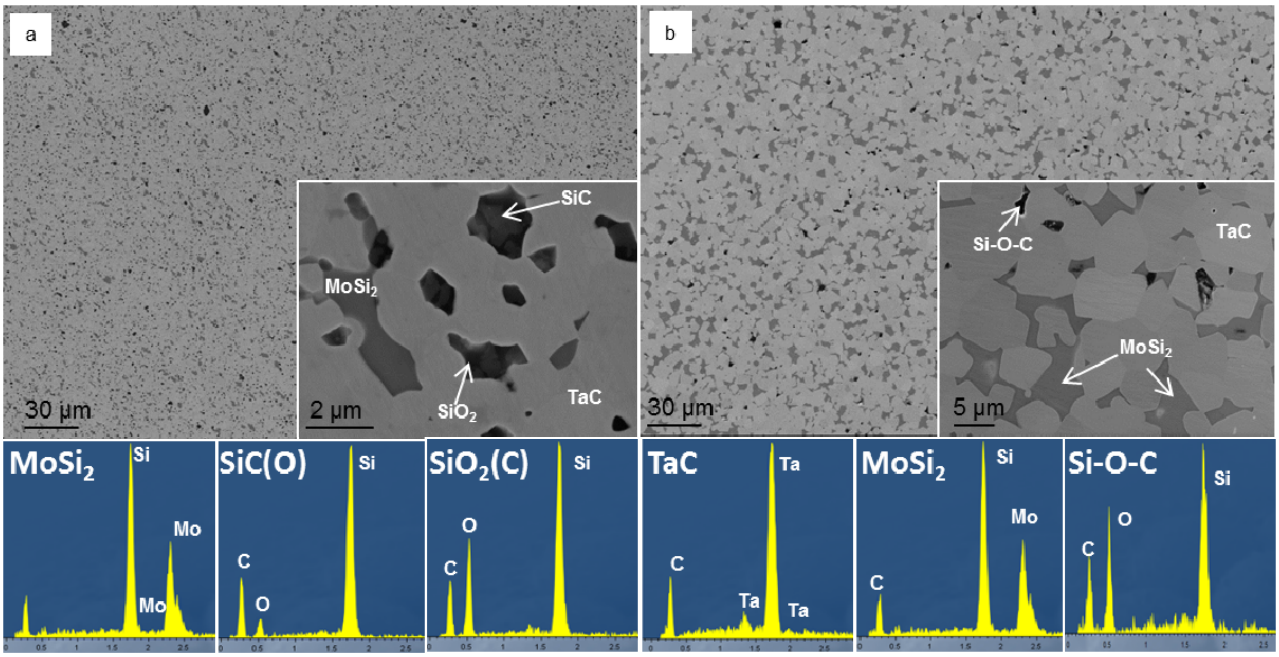

Figure 3: *SEM images of the microstructure of TaC-based composites sintered by a) hot pressing and 10 vol% of $MoSi_2$ and b) pressureless sintering and 20 vol% of $MoSi_2$ with EDS spectra of the various phases.*

3.2 Surface Roughness

Figure 4 reports the average roughness, Ra, and maximum distance between peak and valley, Rt, for the composites densified by hot pressing and pressureless sintering. It can be read that both plots follow the same trend, therefore, for simplicity, only Ra will be discussed.

In general, hot pressed materials can achieve smoother surfaces, probably owing to a higher relative density and smaller mean grain size, than the corresponding composites sintered without pressure. Ra values are about one order of magnitude lower for HP than for PLS samples, with 1:10 ratio for ZrC and TaC and even higher ratio for HfC, 1:30. As a rule of thumb, PLS materials have the tendency to exhibit surface roughness Ra ≥10 nm Rt ≥0.2 μm, HP samples have Ra <5 nm, Rt<0.2 μm.

Paper published on:
Solar Energy vol. 131 (2016), pages: 199–207
DOI: 10.1016/j.solener.2016.02.045
http://www.sciencedirect.com/science/article/pii/S0038092X16001547

Inside the hot pressed class of materials, TCM and HCM with comparable mean grain size (1.5 μm) and residual porosity (<0.5%), have similar Ra, whilst Ra for HP ZCM is higher probably due to larger mean grain size (5 μm), in agreement with that observed for other types of materials [26]

As for pressureless sintered materials, the low value for Ra for TCM is related to the low amount of residual porosity. Ra of HCM is instead strongly affected by 12% of surface porosity resulted from grains pullout. For ZCM, Ra is increased either by some residual porosity and larger mean grain size (see Table I).

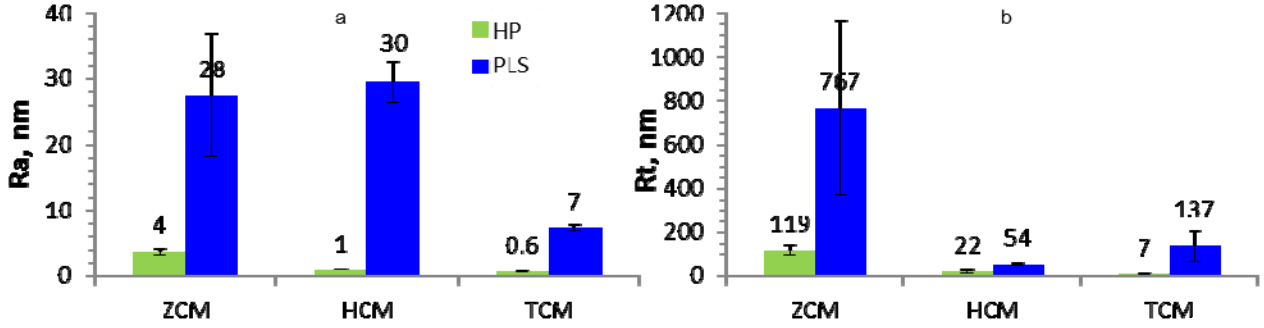

Figure 4: *Plots of a) average roughness, Ra, and b) maximum distance between peak and valley, Rt, for the carbides densified by hot pressing (HP) and pressureless sintering (PLS).*

3.3 Basic mechanical properties

The measured mechanical properties for the UHTCs in exam are reported in Table I. Hot pressed materials are characterized by a higher strength than the corresponding pressureless-sintered compositions. This feature is not strictly related to the amount of $MoSi_2$, but rather to the kind of process used. Compared to conventional sintering, hot pressing allows reaching a higher density and finer grain size, with a reduction of the defects population. This, in turn, results in improved strength [23, 24]. The same trend holds for high temperature values, which, in the case of carbides, are always lower than room temperature ones. After tests at 1500 K, the bars showed microstructural alteration due to oxidation [23, 24]. This indicates that despite the presence of a protective Ar flux, residual oxygen reacted with the ceramics. Strength decay at high temperature is hence attributed to partial oxidation.

For both hot pressed and pressureless sintered samples, it can be noticed that TaC-based materials have superior performance compared to HfC and ZrC, both at room and high temperature. ZrC – based materials are affected by larger mean grain size of the starting powder which results in coarsened microstructures of the sintered materials. On the other hand, HfC-based carbides are affected by extra amount of HfO_2 deriving from oxygen contamination of the starting HfC powder (0.35 wt%).

3.4 Optical spectra

Figure 5 compares the 10 vol% $MoSi_2$ and 20 vol% $MoSi_2$ samples for the different materials. We can appreciate that for both investigated classes (10 and 20 vol% containing $MoSi_2$, corresponding to HP and PLS fabrication processes, respectively), reflectance decreases from TaC to ZrC to HfC. This trend is in agreement with previous studies and is related to the intrinsic radiative properties of the three carbides. For instance, the higher reflectance of ZrC compared to

Paper published on:
Solar Energy vol. 131 (2016), pages: 199–207
DOI: 10.1016/j.solener.2016.02.045
http://www.sciencedirect.com/science/article/pii/S0038092X16001547

HfC is consistent with lower emissivity of the former measured at higher temperature, as found both by our and other groups [17, 27].

Even if the detailed theoretical interpretation of optical features is out of the scope of the present work, we can make some basics comments. In fact, the electronic band structure of carbides allows explaining the main characteristics of the observed optical spectra (e.g. the effects of the sample primary phase). However, it should be emphasized that these considerations are forced to be only qualitative, as defect states due to deviations from stoichiometry and grain boundaries strongly affect the resulting density of states [28, 29]. For instance, the observed high reflectance plateau at long wavelengths is connected to intra-band transitions and described by the Drude model in metal-like materials, while inter-band transitions effects account for the dip in the reflectivity curves [29] and are typically located at lower energies for ZrC and HfC [29] than for TaC [30], thus explaining the relatively better radiative properties of the latter. The similarity between the electronic density of states of hafnium and zirconium compounds [29] explains the similarity between the spectra of pure ZrC and HfC [13]. In our samples this can be recognized in 10 vol%-doped specimens, while, in the 20 vol% ones, it is lost because of roughness/porosity and composition effects, as explained below.

As for the effects of surface roughness, it can be observed that the lower Ra found for TaC-based materials is an additional factor explaining the higher reflectance of these ceramics compared to HfC and ZrC. Again, the effect of surface roughness can be observed in the spectra of PLS samples, for HfC. In this case, the superficial porosity (12%) notably increased Ra and decreased the reflectance with respect to the corresponding HP samples.

From peculiar features of the spectra, it is possible to infer some compositional information of investigated surfaces. For instance, the presence of $MoSi_2$ in the samples can be recognized from the reflectivity minimum at around 2.7 μm, as confirmed by previous studies [12]. This minimum is obviously more pronounced for compositions with 20 vol%, rather than for 10 vol% (Figure 6) and is more evident for TaC-based composites. Indeed, we should consider that the initial nominal content of $MoSi_2$ is strongly changed after sintering, due to partial conversion of $MoSi_2$ to SiC. In this respect, according to Table I, TaC-based compositions are those containing the highest amount of residual $MoSi_2$ and PLS TCM20 has the highest content. For HfC -based ceramics, the presence of the 2.7 μm shoulder is not very visible due to removal of $MoSi_2$ phase on the surface. On the other hand, the spectral signature of SiC can be often, but not always, recognized by a feature at around 12 μm, corresponding to its known Reststrahlen peak [31] and it has been evidenced mainly in ZCM10 and HCM10, in agreement with microstructural analysis (Fig. 1, 2a). Generally speaking the identification of this peak is not always possible, and a content of 5 vol% seems to be the minimum detectable level in these ceramics. For instance, despite the presence of 5 vol% SiC in ZCM20, the corresponding peak in the spectrum was not recorded. This could be due to several reasons including the fact that, in this sample, SiC particles had bigger size, but were dispersed discontinuously, compared to ZCM10 where SiC was much finer and homogeneously scattered throughout the surface.

To sum up, although the present study deals with three types of carbides where different variables are changing (mean grain size, secondary phase, surface roughness), we can gather a general trend: optical spectra are chiefly affected by the intrinsic radiative properties of the ceramics. The second fundamental parameter affecting the optical spectrum seems to be the surface roughness, even though it does not impact on the hierarchy of reflectance among different materials. Surface roughness is mainly related to the surface porosity, which in turn is determined by the kind of process used. Hot pressed materials are always denser than pressureless ones, thus having a lower roughness and a higher reflectance.

Paper published on:

Solar Energy vol. 131 (2016), pages: 199–207
DOI: 10.1016/j.solener.2016.02.045
http://www.sciencedirect.com/science/article/pii/S0038092X16001547

The amount of $MoSi_2$ is also expected to affect reflectance significantly. Ongoing studies on hot pressed materials with increasing amounts of $MoSi_2$ have shown that reflectance has the tendency to increase with decreasing the $MoSi_2$ amount. Thus, for hot pressed samples with 10 vol% $MoSi_2$, the reflectance is always higher than PLS samples with 20 vol% $MoSi_2$ due to both decrease of surface roughness and less residual $MoSi_2$ content after sintering (see Table 1).

Other parameters, such as secondary phases in amounts lower than 5-8% and mean grain size do not seem to have an appreciable effect.

Compared to the ideal behavior of a solar absorber (e.g. reflectance is 0 below 1.5 μm and 100% at longer wavelengths) if we consider for instance a working temperature of 1200 K, we can say that TaC-based composites are the best amongst the composition investigated, being intrinsically selective in a higher extent compared to HfC and ZrC (see below). Additional factors to consider for increasing the reflectance are both a minimization of the final porosity and a reduction of the surface roughness as much as possible. As for the secondary phase, the addition of $MoSi_2$ sintering aid should be minimized to avoid the formation of the 2.7 μm shoulder.

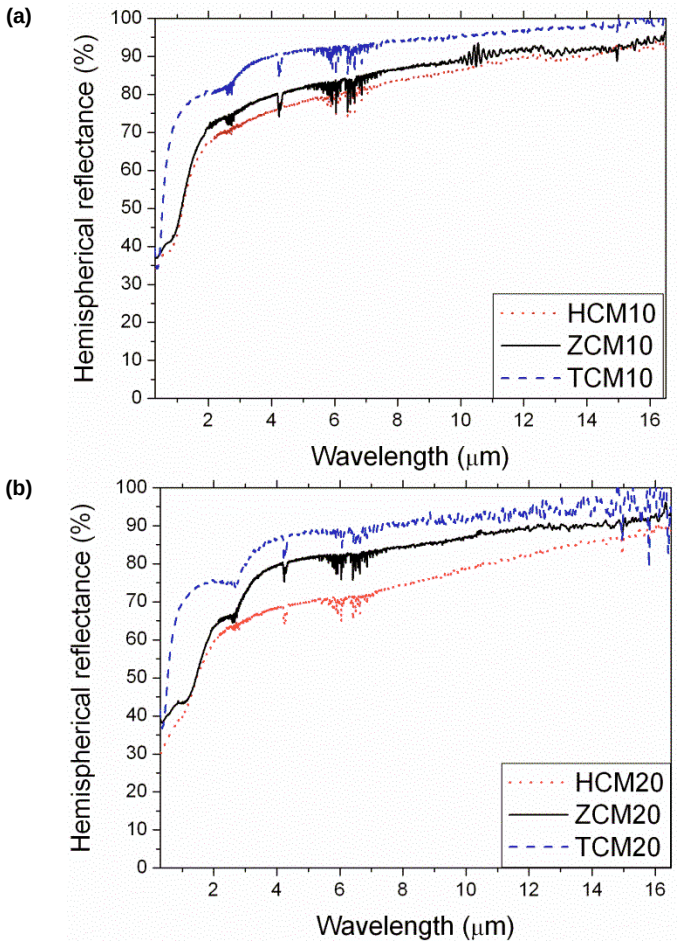

Figure 5: *Comparison of hemispherical reflectance spectra of different materials for fixed sintering aid content.*

Figure 6 compares, for each fixed material, the hemispherical reflectance spectra as a function of the amount of sintering aid. We should notice that hot pressed specimens (10 vol% $MoSi_2$), which always have the highest density, the lowest roughness and the smallest grains, always show also the highest reflectance when compared to PLS samples. The reflectance hierarchy

Paper published on:
Solar Energy vol. 131 (2016), pages: 199–207
DOI: 10.1016/j.solener.2016.02.045
http://www.sciencedirect.com/science/article/pii/S0038092X16001547

is clear for wavelength above about 1 µm. The slightly higher reflectance at shorter wavelengths of TCM20 and ZCM20 samples compared to TCM10 and ZCM10, respectively, is not significant as it lies within the instrumental uncertainty (1-2% in absolute reflectance). As mentioned above, the small curve feature at around 12 µm in ZCM10 and HCM10 can be ascribed to the detection of SiC secondary phase, as it is confirmed by microstructural analysis, while the shoulder at around 2.5 µm in ZrC and TaC-based samples can be explained in terms of $MoSi_2$ residuals. In agreement with the microstructural observations, $MoSi_2$ signal is not detected in HfC-based materials, Fig. 6b.

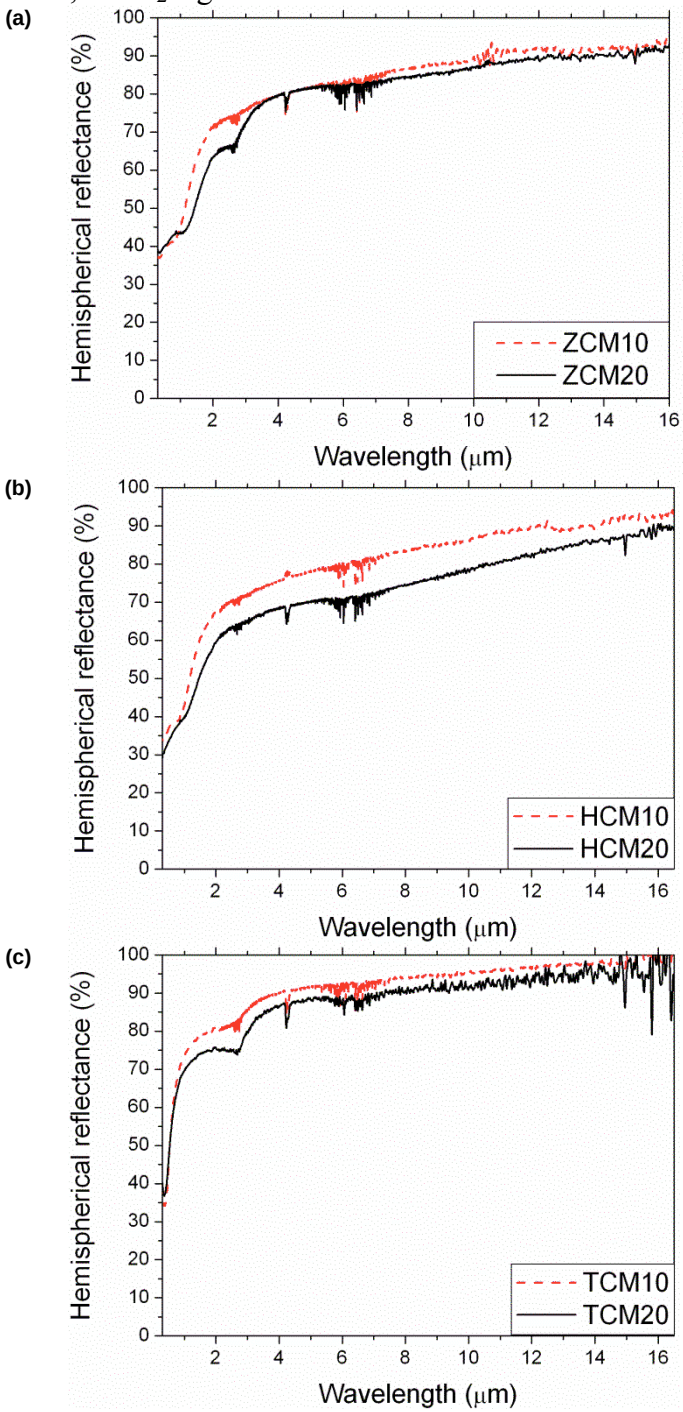

Figure 6: *Comparison of hemispherical reflectance spectra of different materials as a function of the additive amount.*

Paper published on:

Solar Energy vol. 131 (2016), pages: 199–207
DOI: 10.1016/j.solener.2016.02.045
http://www.sciencedirect.com/science/article/pii/S0038092X16001547

From the experimental room-temperature hemispherical reflectance $\rho^{\frown}(\lambda)$ we calculated both the total solar absorbance, α, and an estimated hemispherical emittance, ε, at 1200 K according to the equations:

$$\alpha = \frac{\int_{\lambda_{min}}^{\lambda_{max}} (1-\rho^{\frown}(\lambda)) \cdot S(\lambda) d\lambda}{\int_{\lambda_{min}}^{\lambda_{max}} S(\lambda) d\lambda} \qquad (1)$$

where S(λ) is the Sun emission spectrum [32] and the integration is carried out between λ_{min}=0.3 μm and λ_{max}=2.3 μm; and:

$$\varepsilon = \frac{\int_{\lambda 1}^{\lambda 2} (1-\rho^{\frown}(\lambda)) \cdot B(\lambda,1200K) d\lambda}{\int_{\lambda 1}^{\lambda 2} B(\lambda,1200K) d\lambda} \qquad (2)$$

where B(λ,1200K) is the blackbody spectral radiance at 1200K temperature and λ1=0.3 μm and λ2=15.0 μm. Qualitatively speaking, Eqs. (1) and (2) show that a low ε is connected to a high reflectance at mid infrared wavelengths, while a high α relies on a low reflectance in the visible and near infrared. As briefly discussed above, a high mid-IR reflectance plateau and moderate reflectance values at visible-near IR wavelengths are characteristics of metal-like compounds, with differences among them due to the detail of the electronic structure.

The α/ε ratio (also called spectral selectivity) is a parameter assessing the material potential for solar receiver applications, and ideally should be taken as higher as possible. In fact, it is established that spectral selectivity is a key parameter for increasing the efficiency of solar thermal systems [21]. In addition to that, it should be also mentioned the importance of a high solar absorbance, which represents, on the other hand, a possible criticism for UHT carbides, as this property is generally lower, for instance, than that of silicon carbide (SiC). However, it has been recently demonstrated, for the case of hafnium carbide [33] that solar absorbance can be significantly increased by surface texturing without detrimentally affecting thermal emittance. Table II lists the calculated α and ε values and their ratio. While the absorbance value remains in all cases to be improved, for instance using femtosecond laser writing as described in [33], or chemical attack techniques similar to those used for black silicon [34], the absorbance is higher for 20 vol%-$MoSi_2$ specimens and for HfC-based material (0.61).

As for spectral selectivity, 10 vol% $MoSi_2$-containing specimens (i.e. HP materials) are more performing among all the three investigated carbides, while, for fixed sintering aid amount, the best performing material is always TaC and the worse is HfC. However, three samples (HCM10, TCM20 and ZCM20) share similar α/ε values (2.2, 2.2 and 2.1, respectively). The lowest obtained value is for HCM20 (1.8), but it is not an unfavourable result, as, in any case, it is nearly twice that of the reference SiC (1.0) [14].

Paper published on:

Solar Energy vol. 131 (2016), pages: 199–207
DOI: 10.1016/j.solener.2016.02.045
http://www.sciencedirect.com/science/article/pii/S0038092X16001547

Sample	α	ε	α/ε
HCM10	0.57	0.26	2.2
HCM20	0.61	0.34	1.8
TCM10	0.37	0.13	2.8
TCM20	0.39	0.18	2.2
ZCM10	0.55	0.23	2.4
ZCM20	0.56	0.27	2.1

Table II: *Calculated solar absorbance, thermal emittance and α/ε ratios.*

Conclusions

In this work we systematically compared three ultra-high temperature carbide matrices (ZrC, HfC and TaC) produced by high pressure (HP) and pressureless (PLS) sintering techniques and containing 10 and 20 vol% of $MoSi_2$ sintering aid, respectively. Final compositions, in particular matrix grain size, type and amount of secondary phases, are quite different from the nominal ones and are strongly affected by the sintering process.

HP specimens typically reach slightly higher densities than the corresponding PLS samples, as well as smaller grain size, smoother surface, higher fracture strength and better spectral selectivity (higher α/ε ratio). For fixed processing technique, the best optical characteristics are shown by TaC and the worst by HfC. Compared to the ideal behavior of a solar absorber, we can say that TaC-based composites are the best amongst the composition investigated, also in terms of mechanical performance.

From the point of view of optical properties, the addition of $MoSi_2$, although necessary to enable densification and provide SiO_2-glass upon oxidation, should be kept as lower as possible to decrease the shoulder at 2.7 μm which is detrimental for thermal emittance. However, even the worst spectrally performing material, i.e. HfC produced by PLS, can be favorably compared to the reference silicon carbide, as its α/ε ratio is nearly twice.

Acknowledgements

Part of this activity has been carried out in the framework of the FIRB2012-SUPERSOLAR project funded by the Italian Ministry of University and Research (Programma “Futuro in Ricerca”, prot. RBFR12TIT1). E. S. gratefully acknowledges the Italian bank foundation “Fondazione Ente Cassa di Risparmio di Firenze” for providing the grant for M.M. within the framework of the “SOLE” and “SOLE-2” projects (pratiche n. 2013.0726 and 2014.0711). Thanks are due to Mr. M. D’Uva and Mr. M. Pucci (CNR-INO) for technical assistance.

References

[1] M. Romero, A. Steinfeld, Concentrating solar thermal power and thermochemical fuels, Energy Environ. Sci., 5 (2012) 9234

[2] S.A. Kalogirou, Solar thermal collectors and applications. Prog Energy Combust Sci 30 (2004) : 231-95.

[3] T. Yan, Y. Chen, Review of study on solid particle solar receivers, Renew. Sust. Energy Rev. 14 (2010) 265-76.

[4] H. Naito, Y. Koshaka, D. Cookie, H. Arashi, Development of a solar receiver for a high-efficiency thermionic/Thermoelectric conversion system, Solar Energy 58 (1996) 191-5

[5] J. Capeillère, A. Toutant, G. Olalde, A. Boubault, Thermomechanical behavior of a plate ceramic solar receiver irradiated by concentrated sunlight, Solar Energy 110 (2014) 174–187

Paper published on:

Solar Energy vol. 131 (2016), pages: 199–207
DOI: 10.1016/j.solener.2016.02.045
http://www.sciencedirect.com/science/article/pii/S0038092X16001547

[6] T. Fend, R. Pitz-Paal, O. Reutter, J . Bauer, B. Hoffschmidt, Two novel high-porosity materials as volumetric receivers for concentrated solar radiation, Solar Energy Materials & Solar Cells 84 (2004) 291–304
[7] I. Hischier, P. Pozivil, A. Steinfeld, A Modular Ceramic Cavity-Receiver for High-Temperature High-Concentration Solar Applications, Journal of Solar Energy Engineering, Vol. 134 (2012) 011004
[8] S. Mey, C. Caliot, G. Flamant, A. Kribus, Y. Gray, Optimization of high temperature SiC volumetric solar absorber, Energy Procedia 49 (2014) 478 – 487
[9] J. Karni, A. Kribus, R. Rubin, P. Doron, The "porcupine": a novel high-flux absorber for volumetric solar receivers,J. Solar Energy Eng. 120 (1998), 85-95
[10] E. Sani, L. Mercatelli, F. Francini, J.-L. Sans, D. Sciti "Ultra-refractory ceramics for high-temperature solar absorbers", Scripta Materialia, vol. 65, pp. 775–778 (2011)
[11] E. Sani, L. Mercatelli, D. Fontani, J.L. Sans, D. Sciti " Hafnium and Tantalum Carbides for high temperature solar receivers", Journal of Renewable and Sustainable Energy vol. 3, 063107 (2011)
[12] E. Sani, L. Mercatelli, P. Sansoni, L. Silvestroni, D. Sciti, "Spectrally selective ultra-high temperature ceramic absorbers for high-temperature solar plants", Journal of Renewable and Sustainable Energy, vol. 4, 033104 (2012),
[13] E. Sani, L. Mercatelli, D. Jafrancesco, J.-L. Sans, D. Sciti, "Ultra-High Temperature Ceramics for solar receivers: spectral and high-temperature emittance characterization", Journal of the European Optical Society: Rapid Publication, vol. 7, 12052 (2012)
[14] D. Sciti, L. Silvestroni, L. Mercatelli, J.L. Sans, E. Sani, "Suitability of ultra-refractory diboride ceramics as absorbers for solar energy applications", Solar Energy Materials and Solar Cells, vol. 109, pp. 8-16 (2013)
[15] E. Sani, L. Mercatelli, J.L. Sans, L. Silvestroni, D. Sciti, "Porous and dense Hafnium and Zirconium Ultra-High Temperature Ceramics for solar receivers", Optical Materials, vol. 36 (2013), 163–168.
[16] E. Sani, M. Meucci, L. Mercatelli, D. Jafrancesco, J.L. Sans, L. Silvestroni, D. Sciti, "Optical properties of boride ultrahigh-temperature ceramics for solar thermal absorbers", Journal of Photonics for Energy, vol. 4 (2014), 045599.
[17] D. Sciti, L. Silvestroni, J-L. Sans, L. Mercatelli, M. Meucci, E. Sani, Tantalum diboride-based ceramics for bulk solar absorbers, Solar Energy Materials and Solar Cells, 130 (2014), 208-213
[18] D. Sciti, L. Silvestroni, D.M. Trucchi, E. Cappelli, S. Orlando, E. Sani, Femtosecond laser treatments to tailor the optical properties of hafnium carbide for solar applications, Solar Energy Materials & Solar Cells 132 (2015) 460–466.
[19] E. Sani, L. Mercatelli, J.L. Sans, D. Sciti, Optical properties of black and white ZrO_2 for solar receiver applications, Solar Energy Materials and Solar Cells, 140 (2015) 477–482.
[20] L. Weinstein, D. Kraemer, K. McEnaney, G. Chen, Optical cavity for improved performance of solar receivers in solar-thermal systems, Solar Energy 108 (2014) 69–79.
[21] K. Burlafinger, A. Vetter, C. J. Brabec, Maximizing concentrated solar power (CSP) plant overall efficiencies by using spectral selective absorbers at optimal operation temperatures, Solar Energy 120 (2015) 428-438
[22] A. Bellucci, P. Calvani, E. Cappelli, S. Orlando, D. Sciti, R. Yogev, A. Kribus, D. M. Trucchi; "Preliminary characterization of ST2G: Solar thermionic-thermoelectric generator for concentrating systems", 2015/6/23, NANOFORUM 2014 Conference Proceedings, 1667 (2015) 020007

Paper published on:

Solar Energy vol. 131 (2016), pages: 199–207
DOI: 10.1016/j.solener.2016.02.045
http://www.sciencedirect.com/science/article/pii/S0038092X16001547

[23] D. Sciti, L. Silvestroni, S. Guicciardi, D. dalle Fabbriche, A. Bellosi, Processing, mechanical properties and oxidation behavior of TaC and HfC composites containing 15 vol% $TaSi_2$ or $MoSi_2$, J. Of Mat. Res, 25, 6, 2056-65 (2009).
[24] L. Silvestroni, D. Sciti, Sintering Behavior, Microstructure, and Mechanical Properties: A Comparison among Pressureless Sintered Ultra-Refractory Carbides, Advanced in Materials Science and Engineering, vol. 2010, article ID 835018, 11 pages.
[25] L. Silvestroni, D. Sciti, "Microstructure and properties of pressureless sintered ZrC-based materials", Journal of Materials Research 26 [7] 1882-1889 (2008).
[26] J. Kaufman, H. Padamsee, "Surface Roughness vs. Grain Size Analysis on Nb Samples", 12th International Workshop on RF Superconductivity, Cornell University, 2005
[27] A. I. Fisenko, V. Lemberg, Radiative properties of stoichiometric Hafnium, titanium and zirconium carbides: Thermodynamics of thermal radiation, Int. J Thermophys (2012) 33:513-527
[28] A. Modine, T. W. Haywood, C. Y. Allison, Optical and electrical properties of single-crystalline zirconium carbide, Phys. Rev. B 32 (1985) 7743-7747
[29] A. Delin, O. Eriksson, R. Ahuja, B. Johansson, M. S. S. Brooks, T. Gasche, S. Auluck, J. M. Wills, Optical properties of the group-IVB refractory metal compounds, Phys. Rev. B 54 (1996) 1673-1681
[30] F. A. Modine, R. W. Major, T. W. Hatwood, G. R. Gruzalski, D. Y. Smith, Optical properties of tantalum carbide from the infrared to the near ultraviolet, Phys. Rev. B 29 (1984) 836-841
[31] C.F.Bohren, D.R.Huffman, Absorption and Scattering of Light by Small Particles, Wiley,NewYork,1983, page 243
[32] Solar Spectral Irradiance, CIE (Commission Internationale de l'Eclairage), Technical Report no.85, 1989.
[33] D. Sciti, L. Silvestroni, D.M. Trucchi, E. Cappelli, S. Orlando, E. Sani, Femtosecond laser treatments to tailor the optical properties of hafnium carbide for solar applications, Solar Energy Materials & Solar Cells 132 (2015) 460–466
[34] H. M. Branz, V. E. Yost, S. Ward, K. M. Jones, B. To, P. Stradins, Nanostructured black silicon and the optical reflectance of graded-density surfaces, Applied Physics Letters 94 (2009) 231121